JACS
JOURNAL OF THE AMERICAN CHEMICAL SOCIETY

ARTICLE

pubs.acs.org/JACS

Systematic Study of Protein Detection Mechanism of Self-Assembling ^{19}F NMR/MRI Nanoprobes toward Rational Design and Improved Sensitivity

Yousuke Takaoka,[†] Keishi Kiminami,[†] Keigo Mizusawa,[†] Kazuya Matsuo,[†] Michiko Narazaki,[‡] Tetsuya Matsuda,[‡] and Itaru Hamachi*[,†,§]

[†]Department of Synthetic Chemistry and Biological Chemistry, Kyoto University, Katsura, Nishikyo-Ku, Kyoto 615-8510, Japan

[‡]Department of Systems Science, Graduate School of Informatics, Kyoto University, 36-1 Yoshida-Honmachi, Sakyo-ku, Kyoto 606-8501, Japan

[§]Japan Science and Technology Agency, CREST, 5 Sanbancho, Chiyoda-ku, Tokyo 102-0075, Japan

Supporting Information

ABSTRACT: ^{19}F NMR/MRI probe is expected to be a powerful tool for selective sensing of biologically active agents owing to its high sensitivity and no background signals in live bodies. We have recently reported a unique supramolecular strategy for specific protein detection using a protein ligand-tethered self-assembling ^{19}F probe. This method is based on a recognition-driven disassembly of the nanoprobes, which induced a clear turn-on signal of ^{19}F NMR/MRI. In the present study, we conducted a systematic investigation of the relationship between structure and properties of the probe to elucidate the mechanism of this turn-on ^{19}F NMR sensing in detail. Newly synthesized ^{19}F probes showed three distinct behaviors in response to the target protein: off/on, always-on, and always-off modes. We clearly demonstrated that these differences in protein response could be explained by differences in the stability of the probe aggregates and that "moderate stability" of the aggregates produced an ideal turn-on response in protein detection. We also successfully controlled the aggregate stability by changing the hydrophobicity/hydrophilicity balance of the probes. The detailed understanding of the detection mechanism allowed us to rationally design a turn-on ^{19}F NMR probe with improved sensitivity, giving a higher image intensity for the target protein in ^{19}F MRI.

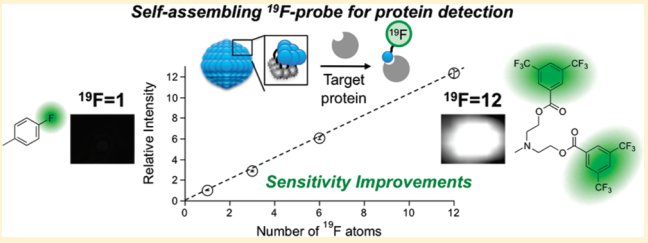

INTRODUCTION

Chemical probes for selective sensing and detection of biologically active molecules have attracted a great deal of attention, not only in basic biological research but also in medical diagnosis and pharmaceutical applications.[1−4] Protein is one of the most important targets among a variety of biomarkers, and chemical probes for versatile and convenient detection or imaging of proteins are in high demand. However, development of protein-specific chemical probes is generally difficult due to the complicated 3D structures of proteins with diverse functions. Recently, Rotello and co-workers[5] and Thayumanavan and co-workers[6] have independently proposed supramolecular approaches to protein detection using amphiphilic polymers or dendrons, showing that such nanomaterials have the potential for use in protein sensing and profiling applications. We also recently reported a unique supramolecular strategy for protein detection using protein ligand-tethered self-assembling nanoprobes.[7,8] This technique is based on a protein-recognition-driven disassembly of the nanoprobes, which produced a clear turn-on signal of ^{19}F NMR/MRI or fluorescence in the detection modality (Figure 1a). Among many detection modalities, MRI is advantageous for deep-tissue and noninvasive imaging in vivo.[9] ^{19}F MRI is anticipated to be a promising alternative to conventional ^{1}H MRI because of its high sensitivity (83% relative to ^{1}H) and no background signals in animal bodies.[10] However, successful examples of the application of ^{19}F-based chemical probes for specific protein detection have been very limited,[11] and thus the development of functional ^{19}F probes is now highly desirable.

Here we describe a systematic structure−property relationship study for elucidating the mechanism of turn-on ^{19}F NMR sensing using the newly synthesized ^{19}F probe derivatives with varying self-assembling properties. Interestingly, in addition to the turn-on probes, we found that some probes gave the ^{19}F NMR signal both in the absence and in the presence of the target protein, indicating that they were always-on probes. Furthermore, some probes produced no signals regardless of the target was present; therefore, these were classified as always-off probes. We clearly demonstrated that the response was strongly controlled by the stability of the self-aggregates in aqueous solution,

Received: April 30, 2011
Published: June 23, 2011

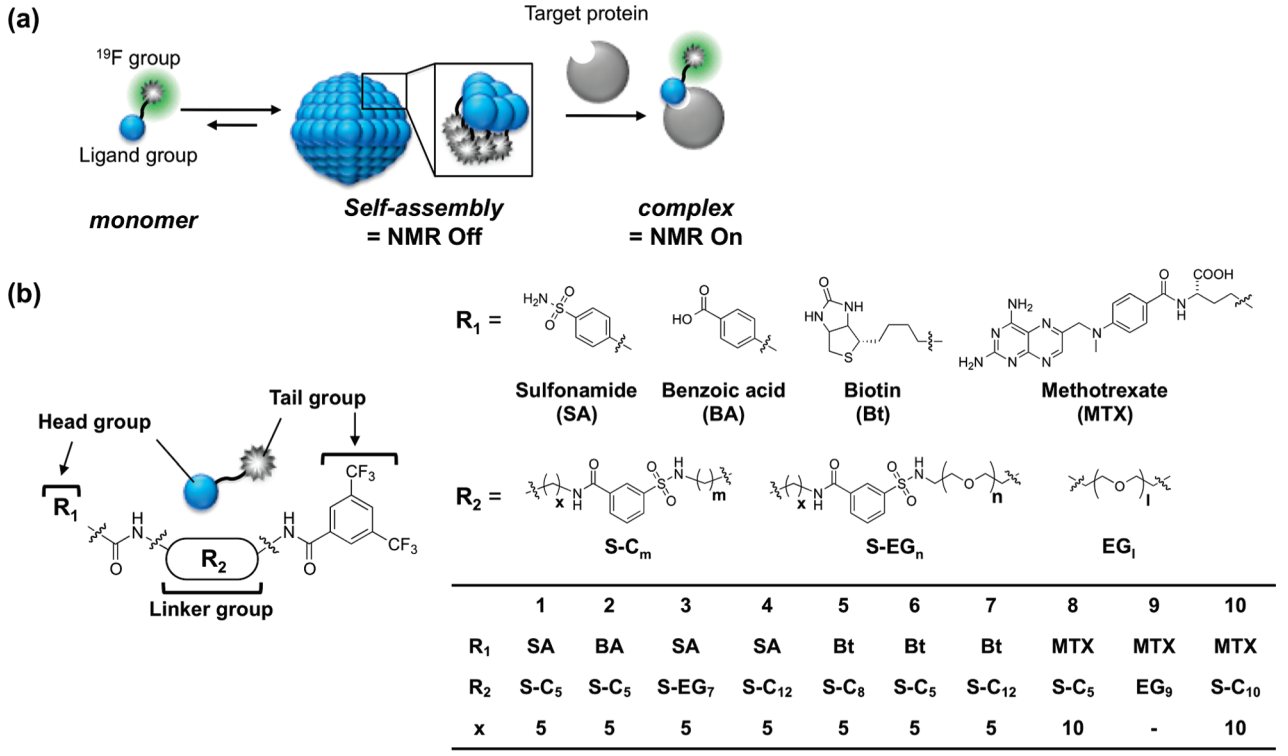

	1	2	3	4	5	6	7	8	9	10
R_1	SA	BA	SA	SA	Bt	Bt	Bt	MTX	MTX	MTX
R_2	S-C_5	S-C_5	S-EG_7	S-C_{12}	S-C_8	S-C_5	S-C_{12}	S-C_5	EG_9	S-C_{10}
x	5	5	5	5	5	5	5	10	-	10

Figure 1. (a) Schematic of self-assembling ^{19}F NMR off/on probe for protein detection. (b) Chemical structures of probes used in this study: **1**, **3**, and **4** for human carbonic anhydrase I (hCAI), **5**−**7** for avidin, **8**−**10** for dihydrofolate reductase (DHFR), and **2** for pH-sensitive probe.

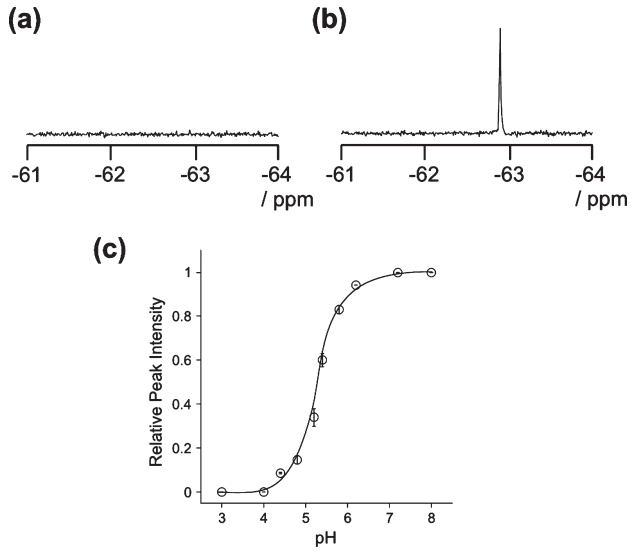

Figure 2. (a, b) ^{19}F NMR spectra of pH-sensitive off/on probe **2** (100 μM) at (a) pH 3.0 or (b) pH 8.0 in a citrate/phosphate buffer system of constant ionic strength[12] [0.5 ion strength, 0.2 mM TFA, 10% D_2O (v/v), 500 μL]. (c) pH profile of signal intensity change of probe **2** was assessed in the same system as shown in panels a and b (trifluoroacetic acid, TFA, was used for an internal standard for signal intensity). Experiments were performed in triplicate to obtain mean and standard deviation values (shown as error bars).

which was modulated by the hydrophilicity/hydrophobicity balance of the probe molecules. The present mechanistic understanding enabled us to design self-assembling probes with improved signal/noise ratio, to afford enhanced sensitivity and brighter ^{19}F MRI in the turn-on detection mode.

RESULTS AND DISCUSSION

^{19}F NMR Signal Intensity Influenced by Hydrophilicity of the Head Group. We initially noticed that the signal-off or -on of ^{19}F NMR is highly dependent on the hydrophilicity of the ^{19}F-tethered molecule when we measured the ^{19}F NMR of a pH-sensitive amphiphilic molecule **2** (Figure 1b), with a structure similar to the ideal off/on probe **1**. The benzoic acid head group of **2** is neutral at acidic pH, whereas it is negatively charged as benzoate at basic pH. When **2** was dissolved in acidic buffer (pH 3), no ^{19}F signal was observed. In contrast, a sharp signal appeared at −62.9 ppm in basic buffer (pH 8) (Figure 2a,b).[12] It was clear from the pH titration experiment that the ^{19}F NMR signal turned on at approximately pH 5.3, which corresponds to the apparent pK_a of benzoic acid (Figure 2c). The visible absorption spectrum of **2** in acidic buffer showed a broad band around 500−700 nm owing to the visible-light scattering, whereas the solution was not turbid in basic solution (Figure S1a, Supporting Information; the scattering intensity at 600 nm showed an 80-fold decrease relative to that in the acidic buffer). These findings suggested that there are aggregates of **2** in the acidic solution but not in the basic solution. Indeed, atomic force microscopy (AFM) revealed the formation of spherical or oval aggregates of **2** with diameters ranging from 10 to 100 nm (Figure S1b, Supporting Information) in the acidic buffer. Consistently, dynamic light scattering (DLS) measurements in acidic buffer containing **2** showed aggregates with a mean diameter of 13 nm (Figure S1c, Supporting Information), whereas negligible

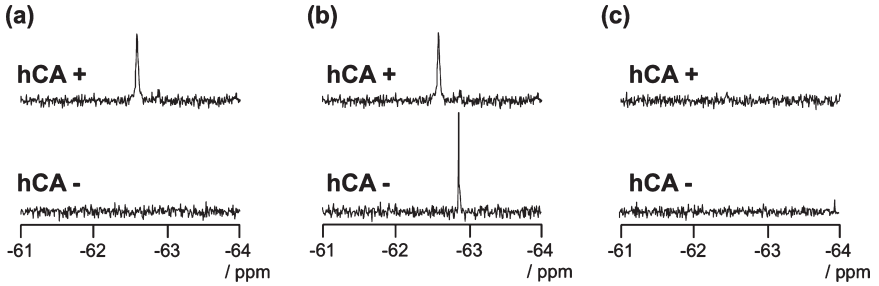

Figure 3. ^{19}F NMR spectra of hCAI-type probes (a) **1**, (b) **3**, and (c) **4** (25 μM), (top) with or (bottom) without 25 μM hCAI, in 50 mM HEPES buffer [pH 7.2, 0.2 mM TFA, 10% D_2O (v/v), 500 μL].

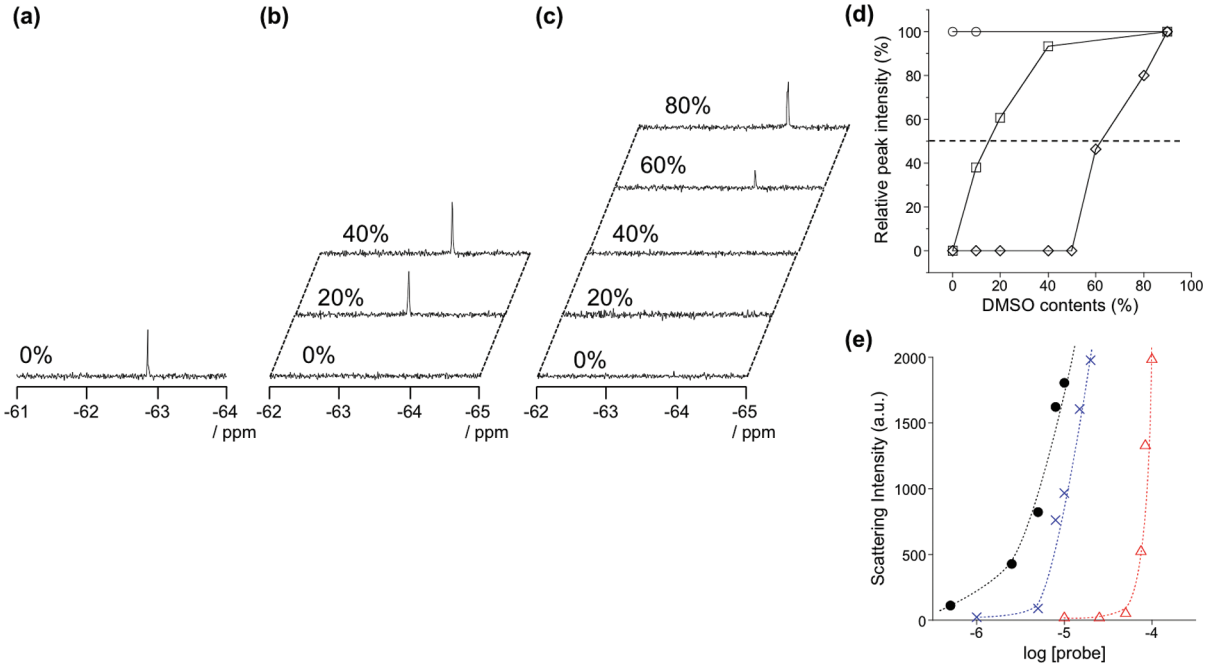

Figure 4. Stabilities of the self-assembling aggregates of probes **3**, **1**, and **4**. (a–c) ^{19}F NMR spectra of probes **3** (a, 25 μM), **1** (b, 25 μM), and **4** (c, 25 μM) in aqueous solution [pH 7.2, 50 mM HEPES buffer (0.2 mM TFA as an internal standard for peak intensity and chemical shift), 500 μL] with various DMSO-d_6 contents. (d) Relative peak intensity changes of probes **3** (○), **1** (□), and **4** (◇) in aqueous solution with various DMSO contents. (e) Concentration-dependent change of scattering intensities of hCAI probes **3** (Δ), **1** (×), and **4** (●) in aqueous solution (pH 7.2, 50 mM HEPES buffer). These intensities were collected from DLS analyses with the same laser intensity and sensitivity.

DLS intensity was obtained in the basic buffer. These results indicate that aggregates of **2** formed in the acidic buffer with protonation of the benzoic acid moiety but they collapsed upon deprotonation in the basic buffer. Aggregation in acidic solution resulted in the apparent molecular mass (M_r) of **2** dramatically increasing from 8×10^2 (monomer) to 5×10^5 Da. It may be reasonable that such an increase in M_r caused a significant increase in the ^{19}F relaxation rate, relative to that in the monomeric form of **2**, affording no NMR signals.[7a] It should be noted that the aggregation/disaggregation was modulated by a change in the hydrophilicity of the head group, which directly led to the disappearance/appearance of the ^{19}F NMR signal.

Three Distinct Response Patterns in Protein Detection via Human Carbonic Anhydrase I ^{19}F Probes. The aggregation property of ^{19}F probes is reasonably considered to be controllable by other modules, as well as the head group, which may influence the turn-on response to a target protein. To examine the effects of the linker module on human carbonic anhydrase I (hCAI) response, we prepared two ^{19}F probes, **3** and **4**, with different linkers based on the structure of the ideal off/on probe **1** for hCAI detection. Our probes consisted of three modules: (i) a hydrophilic ligand specific to a protein of interest (head group, benzenesulfonamide for hCAI),[13] (ii) a hydrophobic 3,5-bis-(trifluoromethyl)benzene for the ^{19}F NMR detection modality (tail group), and (iii) a relatively hydrophobic linker group to connect these two modules (Figure 1b). Interestingly, three different responses to hCAI were found for these probes in the absence and presence of hCAI: off/on, always-on ,and always-off responses. Probe **1** alone was silent in ^{19}F NMR spectroscopy but produced a sharp signal at −62.6 ppm in response to the addition of hCAI (Figure 3a). In contrast, when probe **3**, which has a hydrophilic hepta(ethylene glycol) unit as a linker group, was dissolved in aqueous solution, a sharp ^{19}F signal was observed at −62.9 ppm even without hCAI ("always-on" as shown in Figure 3b).[14] Conversely, probe **4**, which had a hydrophobic alkyl chain linker, gave no ^{19}F signal in the absence or presence

Table 1. Stability Parameters and Response Patterns of Target Protein Detection of ^{19}F NMR Probes 1 and 3 − 10

probe	target protein	HMDC, %	CAC,[a] μM	response patterns
1	hCAI	15	5	off/on
3	hCAI	0	50	always-on
4	hCAI	65	1	always-off
5	avidin	35	5	off/on
6	avidin	2	20	partial always-on[b]
7	avidin	60	1	always-off
8	DHFR	39	2.5	off/on
9	DHFR	0	500	always-on
10	DHFR	59	1	partial always-off[c]

[a] CAC values were determined from concentration-dependent DLS measurements, shown in Figure 4e and Figure S6, Supporting Information. [b] Peak intensity of probe **6** alone was observed no more than 40% relative to the theoretical value in 50 mM HEPES buffer [pH 7.2, 0.2 mM TFA, 10% D_2O (v/v) without NaCl]. [c] Peak intensity of probe **10** recovered only up to 5% by addition of DHFR relative to the theoretical value.

of hCAI ("always-off" as shown in Figure 3c). Undoubtedly, both always-on and always-off responses are not suitable for accurate protein detection. These differences in hCAI response may be explained as follows: probe **3** was too hydrophilic to form stable self-assembling aggregates that are essential for the signal off state, whereas probe **4** formed aggregates that were too robust to undergo the recognition-driven disassembly.

Correlation between Stabilities of Self-Assembling Aggregates and Off/On Response Patterns of ^{19}F Probes. Next, we evaluated the stability of self-assembling aggregates of ^{19}F probes **1**, **3**, and **4** with various measurements. As mentioned above, ^{19}F NMR signals of these probes cannot be observed when they are stably aggregated in aqueous solution, and the signals appear when they are homogeneously dispersed. We attempted to monitor the collapse of the ^{19}F probe aggregates in response to the addition of dimethyl sulfoxide (DMSO) on the basis of disappearance and appearance of ^{19}F NMR signals (Figure 4). As an index of the aggregate stability, the critical DMSO content in aqueous solution that gave the ^{19}F signal appearance at half of the maximum intensity (HMDC) was determined (Figure 4d). The collapse of the aggregates was also confirmed by the decrease in optical density at 600 nm (Figure S2a,b, Supporting Information). The HDMC values for the probes **3**, **1**, and **4** were determined to be 0%, 15%, and 65%, respectively, indicating that the order of the stability of the aggregates is **3** < **1** < **4** (Table 1). Interestingly, these findings are in good agreement with the decrease in hydrophilicity of the linker module of these probes. We also conducted concentration-dependent DLS measurements to determine the critical aggregation concentration (CAC) of these probes, yielding 50, 5, and 1 μM for **3**, **1**, and **4**, respectively (Figure 4e). Clearly, the order of CAC values was well consistent with that of the aforementioned HMDC. Given the stability data among the three probes, we may ascribe the three different responses of the ^{19}F NMR signal to the distinct stability of the self-assembling aggregates. That is, the ^{19}F signal of the always-on type probe **3** appeared even before the addition of hCAI, because the aggregates of **3** were less stable. In contrast, the perfect off/on type probe **1** self-assembled without hCAI and then disassembled in response to hCAI, owing to the moderate stability of the aggregates. Conversely, it was conceivable that aggregates of the always-off type probe **4** were too stable to be disassembled by hCAI recognition. Indeed, we confirmed that the mean diameter of the aggregates **4** did not change substantially in response to the hCAI addition from DLS measurements [97 nm for a buffer solution containing **4** alone and 114 nm after hCAI addition (Figure S2c, Supporting Information)],[15] unlike in the case of the probe **1**. The optical density measurements showed that the scattering of **4** alone in buffer solution was 0.02 at 600 nm, and this value increased slightly in response to the addition of hCAI (Figure S2e, Supporting Information). These findings were in sharp contrast to the behavior of the off/on probe **1**, which showed a 10-fold decrease in response to hCAI addition.[7a] We also confirmed that the enzymatic activity of hCAI was partially inhibited by **4** (Figure S3, Supporting Information), implying that an interaction between **4** and hCAI occurred. These results suggest that the aggregates of **4** did not collapse regardless of the recognition by hCAI; this can be attributed to the high stability of the probes, and therefore, the ^{19}F NMR signals were not observed.

Similar Correlation Observed in Other Self-Assembling Probes. Such a relationship was also observed for other self-assembling probes that detect different proteins in the turn-on mode. The modular design of our probes enables the detection of various target proteins by use of appropriate probes with a hydrophilic head group that has been replaced with a corresponding ligand moiety. We developed two other classes of probes displaying a different ligand group instead of benzenesulfonamide, that is, biotin-tethered probes for avidin[16] (probes **5**−**7**) and probes containing methotrexate (MTX) as a specific inhibitor of dihydrofolate reductase (DHFR)[17] (probes **8**−**10**). As can be inferred from Table 1 and Figure S4 (Supporting Information), always-on and always-off probes were found in both classes of probes, in addition to the turn-on probes. Because the hydrophilicity of the ligand parts differed among probes, the linker structure of the probes that showed the three different responses was varied slightly. For example, the C5 linker gave the turn-on response for the hCAI and DHFR probes (**1** and **8**, respectively), whereas the C8 linker was needed for the turn-on response for avidin (**5**). In the case of avidin probes, probe **6** with the C5 linker exhibited the ^{19}F signal to some extent, indicating that **6** was not a perfect "off/on" probe but rather a partial always-on probe.[18] It should be noted that such a response pattern was closely related to the aggregate stability, which was evaluated on the basis of the HMDC value as in the case of hCAI probes. That is, the HMDC values were 35% and 39% for **5** and **8**, respectively (Figure S5, Supporting Information, and Table 1), which are similar to that of the turn-on probe **1** (15%). On the other hand, the HMDC values were 60% and 59% for always-off probes **7** and **10**, respectively, which are in the same range as that of the always-off probe **4** for hCAI (65%).

Given all data regarding the three off/on probes toward the different target proteins, it is generally accepted that the ^{19}F NMR signal response to a target protein is closely related to the stability of the self-assembling aggregates of the probe. To achieve an ideal turn-on response, moderate stability is crucial, and it can be designed by modulating the hydrophobicity/hydrophilicity balance of ^{19}F probe molecules.

Rational Design of ^{19}F Probe for Enhanced Sensitivity without Loss of Turn-on Mode. Our understanding of the detection mechanism enabled us to design a turn-on ^{19}F NMR/MRI probe with increased sensitivity. It might be simply considered that the sensitivity in ^{19}F NMR is easily improved by

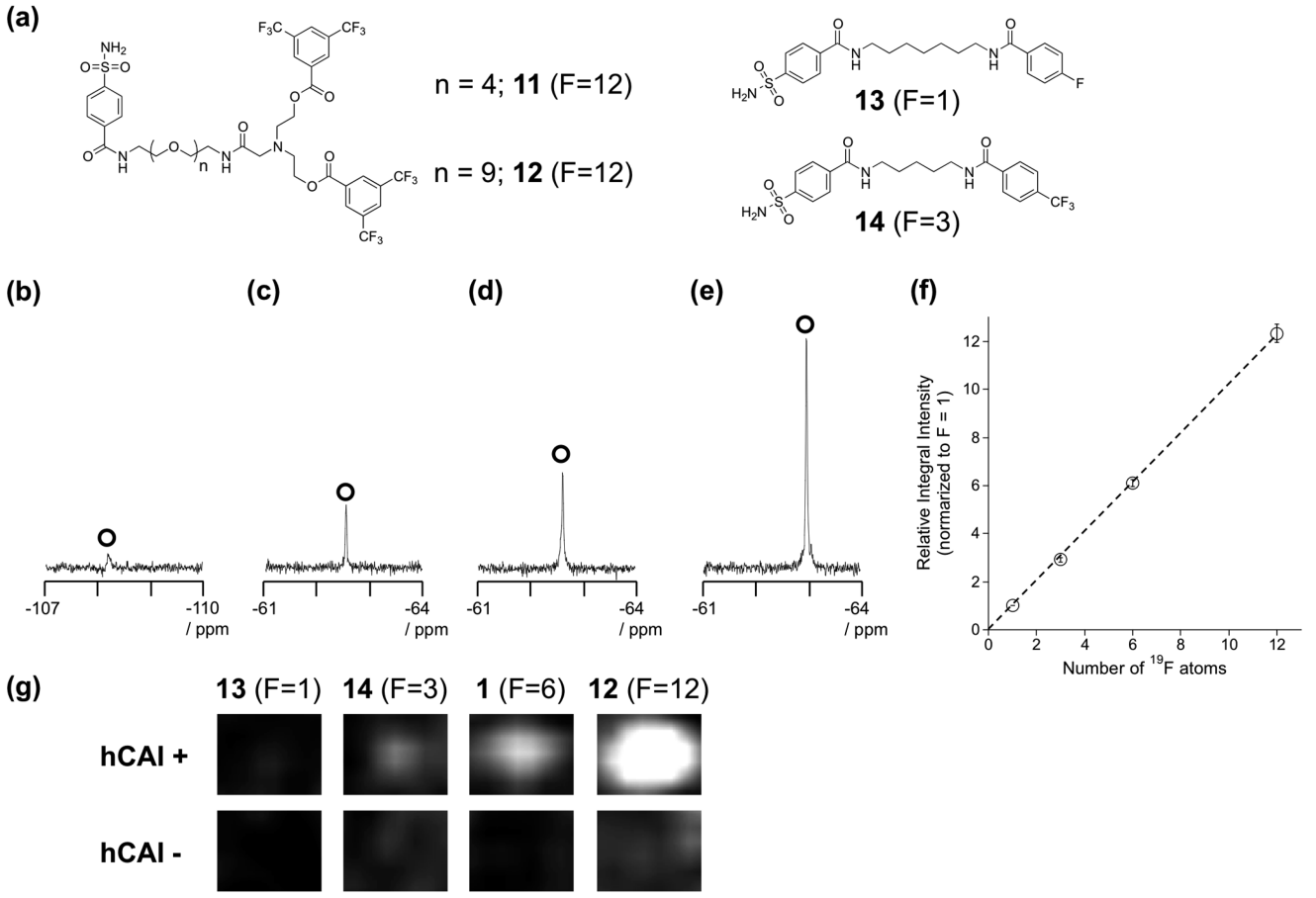

Figure 5. (a) Chemical structures of ^{19}F probes **11**−**14** for hCAI detection. (b−e) ^{19}F NMR spectra of probes (b) **13**, (c) **14**, (d) **1**, and (e) **12** (each concentration was 100 μM) with hCAI (100 μM) in 50 mM HEPES buffer [pH 7.2, 0.2 mM TFA, 10% D_2O (v/v), 500 μL]. (f) Relative integral intensity change with increasing number of ^{19}F atoms in each probes [normalized in probe **13** (^{19}F = 1) in 50 mM HEPES buffer [pH 7.2, 0.2 mM TFA as an internal standard for peak height and chemical shift, 10% D_2O (v/v)]. Experiments were performed in triplicate to obtain mean and standard deviation values (shown as error bars). (g) ^{19}F MR images of probes **13** (F = 1), **14** (F = 3), **1** (F = 6) and **12** (F = 12) (each concentration was 100 μM), (top) with or (bottom) without hCAI (100 μM) in 50 mM HEPES buffer (pH 7.2, 0.2 mM TFA, 2 mL). The signal-to-noise ratios (SNR) were 1.51, 3.42, 5.55, and 9.96 for **13**, **14**, **1**, and **12**, respectively.

increasing the number of ^{19}F nuclei in the probe. However, the stability of the probe aggregates is inevitably enhanced due to the strong hydrophobicity of the additionally incorporated ^{19}F atom, which yields the always-off probe instead of the off/on probe. We thus needed to carefully adjust the aggregates stability by controlling the hydrophilicity of the linker group. In fact, we prepared two new ^{19}F probes (**11** and **12**, Figure 5a) containing twelve ^{19}F nuclei as the dimeric 3,5-bis(trifluoromethyl)benzene unit with tetra- or nona(ethylene glycol) (oligo-EG) linker and examined the off/on response. In both cases, ^{19}F NMR signals were not observed when the probes were dissolved alone in aqueous solution, whereas sharp signals appeared after the addition of hCAI. However, for **11** (4-EG), the ^{19}F signal recovered only up to 50% of its intensity in response to hCAI, probably owing to the rather robust aggregates that were formed. In contrast, we found that almost 100% of the ^{19}F signal was recovered in response to hCAI for probe **12** (9-EG), indicating that the aggregate stability was suitably tuned by the elongated ethylene glycol linker. These response patterns were again explained by the stability of the aggregates. That is, the HMDC value of the off/on probe **12** was 27%, which was similar to that of the ideal off/on probe **1** (15%). On the other hand, the HMDC value of the partial off/on probe **11** was found to be 45%, which was rather close to that of the always-off probe **4** (65%) (Figure S7, Supporting Information). We subsequently compared the off/on ^{19}F signal intensity among four different probes, **13**, **14**, **1**, and **12**, which had one, three, six, and twelve magnetically equivalent ^{19}F nuclei, respectively (Figure 5a). We separately confirmed that all of these were off/on probes for hCAI. As shown in Figure 5b−f, the signal intensity increased linearly as the number of ^{19}F nuclei in these probes increased.[19]

These turn-on ^{19}F NMR probes can visualize the target protein in a ^{19}F MRI phantom, and the above-mentioned sensitivity improvements of our self-assembling ^{19}F probes resulted in clearer MR images. As shown in Figure 5g, the signal intensities of ^{19}F MRI were greatly enhanced and thus the higher image intensity was obtained as the number of ^{19}F nuclei increased for probes **13**, **14**, **1**, and **12**, in the presence of the same concentration of hCAI in each solution. In phantom experiments conducted on our ^{19}F MRI instrument, the minimum times required to obtain clear images (signal-to-noise ratios greater than 2) were 3 h, 1 h, and 10 min for **14**, **1**, and **12**, respectively.[20] These results clearly indicated that the designed probe containing twelve ^{19}F nuclei is indeed able to improve the sensitivity of ^{19}F MRI.

CONCLUSION

In the present systematic structure−property relationship study of our self-assembling ^{19}F NMR/MRI probes, we characterized probes that showed three different behaviors in response to the target protein: off/on, always-on, and always-off types. Through optical density measurements and ^{19}F NMR spectroscopy following the addition of DMSO, these differences in protein responses were found to be closely related to the stability of the probe aggregates. It was clear that the "moderate stability" of the self-assembling aggregates was critical to an ideal turn-on response for protein detection and that the stability could be controlled by altering the hydrophobicity/hydrophilicity balance of the probes. Importance of this balance for efficient protein detection using self-assembling systems was also pointed out by Thayumanavan and co-workers.[6b,c] On the basis of our understanding of the detection mechanism, we successfully designed a turn-on ^{19}F NMR/MRI probe with improved sensitivity. We believe that the present mechanism-based probe design is an important first step toward imaging biologically significant target proteins by use of self-assembling ^{19}F MRI probes in cells or in vivo.

EXPERIMENTAL SECTION

General Materials and Methods. All proteins and chemicals were obtained from commercial suppliers (Sigma, Aldrich, TCI, Wako, or Watanabe Chemical Industries) and used without further purification. ^{19}F NMR spectra were recorded on a JEOL ECX-400P (376.5 MHz) spectrometer and calibrated with TFA (−75.6 ppm). Standard parameters were used with a 36 kHz spectral width, 8 μs pulse length, 0.46 s acquisition time, and 0.50 s relaxation delay. A 0.1 Hz line broadening was applied. The number of accumulations was 1024. UV−visible spectra were recorded on a Shimadzu UV−visible 2550 spectrometer. AFM measurements were performed with a Shimadzu SPM-9600. DLS measurements were performed with a NICOMP 380zls. The scattering angle was 108° and the wavelength of the laser was 520 nm. ^{19}F MR images were obtained on a 7 T Bruker-Biospec 70/20 USR system (282 MHz for ^{19}F) with 72 mm i.d. ^{1}H/^{19}F radio frequency (RF) volume coil (Bruker Biospin, Germany). ^{1}H NMR spectra were recorded on a Varian Mercury-400 (400 MHz). High-resolution fast atomic bombardment mass spectrometry (HR-FAB MS) spectra and high-resolution electrospray ionization quadrupole Fourier transform mass spectrometry (HR-ESI-MS) spectra were performed on a JEOL JMS-HX110A with 3-nitrobenzyl alcohol (NBA) as the matrix and on a Bruker apex-ultra (7 T) mass spectrometer, respectively, by Dr. Keiko Kuwata (Department of Synthetic Chemistry and Biological Chemistry, Graduate School of Engineering, Kyoto University).

Evaluation of hCAI Detection Properties of ^{19}F Probes 1, 3, and 4. hCAI (Sigma, C4396) was dissolved in 50 mM *N*-(2-hydroxyethylpiperazine)-*N*′-2-ethanesulfonic acid (HEPES) buffer [pH 7.2, 10% D_2O (v/v), 0.2 mM TFA, 500 μL]. The concentration of hCAI was determined by measuring the absorbance at 280 nm with the molar extinction coefficient (49 000 $M^{-1}cm^{-1}$),[21] and the stock solution was prepared. ^{19}F probe **1**, **3**, or **4** was dissolved in dimethyl sulfoxide (DMSO) as the stock solution and slowly added to the hCAI solution [0.6% DMSO (v/v)]. These samples were analyzed by ^{19}F NMR spectroscopy with TFA as an internal standard (−75.6 ppm). All the experiments were acquired at 25 °C.

Evaluation of Stabilities of Self-Assembling Aggregates by ^{19}F NMR Spectroscopy. The concentration of ^{19}F probe was fixed at 25 μM in each experiment. The stock solution of each ^{19}F probe was added to the mixed solvent of DMSO-d_6 and 50 mM HEPES buffer (pH 7.2, 0.2 mM TFA). These samples dissolved in arbitrary DMSO contents (0−95%) were analyzed by ^{19}F NMR spectroscopy, and the relative signal intensities of probe itself were compared with TFA (as an internal standard, −75.6 ppm) for calculating the peak recovery ratio against the theoretical value of which whole aggregates dispersed in the solution.

MRI Experiments of ^{19}F Probes 12−14 and 1. The samples were prepared as described in a preceding section, with hCAI (200 μM) and probes (200 μM) (2 mL, depth of sample tube 20 mm). ^{19}F magnetic resonance images of samples were obtained by fast spin echo with repetition time/echo time 1000/5.5 ms, echo train length 32, field of view 24 × 6 cm without slice selection, matrix size 128 × 32, and the number of accumulations 10 800. The excitation pulse width was 1370 Hz. The sine window function was applied to the ^{19}F magnetic resonance images. For determination of the signal-to-noise ratios (SNR), background signal intensity was used as the noise intensity. All the images were acquired at 20 °C.

ASSOCIATED CONTENT

Supporting Information. Seven figures as described in the text, two tables, and additional text and 12 schemes describing experimental details and synthesis procedures. This material is available free of charge via the Internet at http://pubs.acs.org.

AUTHOR INFORMATION

Corresponding Author
ihamachi@sbchem.kyoto-u.ac.jp

ACKNOWLEDGMENT

We thank Dr. S. Tsukiji (Nagaoka University of Technology) for helpful discussion during the early stages of this project. We thank Dr. T. Sera (Kyoto University, Umeda Lab) for help with DLS measurements. We thank Dr. M. Ikeda (Kyoto University, Hamachi Lab) for help with AFM measurements. Y.T., K. Mizusawa, and K. Matsuo acknowledge JSPS Research Fellowships for Young Scientists. This work was partly supported by the CK Integrated Medical Bioimaging Project (MEXT) and CREST (Japan Science and Technology Agency).

REFERENCES

(1) (a) Lavis, L. D.; Raines, R. T. *ACS Chem. Biol.* **2008**, *3*, 142. (b) Haugland, R. P. *The Handbook: A Guide to Fluorescent Probes and Labeling Technologies*, 10th ed.; Invitrogen: Carlsbad, CA, 2005.

(2) (a) Valeur, B.; Leray, I. *Coord. Chem. Rev.* **2000**, *205*, 3. (b) Domaille, D. W.; Que, E. L.; Chang, C. J. *Nat. Chem. Biol.* **2008**, *4*, 168. (c) Kikuchi, K.; Komatsu, K.; Nagano, T. *Curr. Opin. Chem. Biol.* **2004**, *8*, 182.

(3) (a) Kobayashi, H.; Ogawa, M.; Alford, R.; Choyke, P. L.; Urano, Y. *Chem. Rev.* **2010**, *110*, 2620. (b) Kiyose, K.; Kojima, H.; Nagano, T. *Chem.—Asian J.* **2008**, *3*, 506.

(4) (a) Kiessling, F.; Morgenstern, B.; Zhang, C. *Curr. Med. Chem.* **2007**, *14*, 77. (b) Sosnovik, D. E.; Weissleder, R. *Curr. Opin. Biotechnol.*

2007, *18*, 4. (c) Jun, Y. W.; Lee, J.-H.; Cheon, J. *Angew. Chem. Int. Ed.* **2008**, *47*, 5122. (d) Woods, M.; Woessner, D. E.; Sherry, A. D. *Chem. Soc. Rev.* **2006**, *35*, 500.

(5) (a) You, C.-C.; Miranda, O. R.; Gider, B.; Ghosh, P. S.; Kim, I.-B.; Erdogan, B.; Krovi, S. A.; Bunz, U. H. F.; Rotello, V. M. *Nat. Nanotechnol.* **2007**, *2*, 318. (b) De, M.; Rana, S.; Akpinar, H.; Miranda, O. R.; Arvizo, R. R.; Bunz, U. H. F.; Rotello, V. M. *Nat. Chem.* **2009**, *1*, 461. (c) Bajaj, A.; Miranda, O. R.; Kim, I.-B.; Phillips, R. L.; Jerry, D. J.; Bunz, U. H. F.; Rotello, V. M. *Proc. Natl. Acad. Sci. U.S.A.* **2009**, *106*, 10912.

(6) (a) Savariar, E. N.; Ghosh, S.; González, D. C.; Thayumanavan, S. *J. Am. Chem. Soc.* **2008**, *130*, 5416. (b) Azagarsamy, M. A.; Sokkalingam, P.; Thayumanavan, S. *J. Am. Chem. Soc.* **2009**, *131*, 14184. (c) Azagarsamy, M. A.; Yesilyurt, V.; Thayumanavan, S. *J. Am. Chem. Soc.* **2010**, *132*, 4550.

(7) (a) Takaoka, Y.; Sakamoto, T.; Tsukiji, S.; Narazaki, M.; Matsuda, T.; Tochio, H.; Shirakawa, M.; Hamachi, I. *Nat. Chem.* **2009**, *1*, 557. (b) Takaoka, Y.; Sun, Y.; Tsukiji, S.; Hamachi, I. *Chem. Sci.* **2011**, *2*, 511.

(8) Mizusawa, K.; Ishida, Y.; Takaoka, Y.; Miyagawa, M.; Tsukiji, S.; Hamachi, I. *J. Am. Chem. Soc.* **2010**, *132*, 7291.

(9) (a) Louie, A. Y.; Hüber, M. M.; Ahrens, E. T.; Rothbächer, U.; Moats, R.; Jacobs, R. E.; Fraser, S. E.; Meade, T. J. *Nat. Biotechnol.* **2000**, *18*, 321. (b) Perez, J. M.; Josephson, L.; O'Loughilin, T.; Högemann, D.; Weissleder, R. *Nat. Biotechnol.* **2002**, *20*, 816.

(10) (a) Danielson, M. A.; Falke, J. J. *Annu. Rev. Biophys. Biomol. Struct.* **1996**, *25*, 163. (b) Yu, J.; Kodibagkar, V. D.; Cui, W.; Mason, R. P. *Curr. Med. Chem.* **2005**, *12*, 819.

(11) (a) Higuchi, M.; Iwata, N.; Matsuba, Y.; Sato, K.; Sasamoto, K.; Saido, T. C. *Nat. Neurosci.* **2005**, *8*, 527. (b) Yu, J.; Liu, L.; Kodibagkar, V. D.; Cui, W.; Mason, R. P. *Bioorg. Med. Chem.* **2006**, *14*, 326. (c) Mizukami, S.; Takikawa, R.; Sugihara, F.; Hori, Y.; Tochio, H.; Wälchli, M.; Shirakawa, M.; Kikuchi, K. *J. Am. Chem. Soc.* **2008**, *130*, 794.

(12) Elving, P. J.; Markowitz, J. M.; Rosenthal, I. *Anal. Chem.* **1956**, *28*, 1179.

(13) Supuran, C. T. *Nat. Rev. Drug Discovery* **2008**, *7*, 168.

(14) By addition of hCAI, the original signal at −62.9 ppm disappeared and a distinct broad signal appeared at −62.6 ppm (Figure 3b). This chemical shift change clearly indicated that the probe **3** was bound to hCAI, similar to probe **1**. These were supported by the transverse relaxation times (T_2) of probe **3** with or without hCAI (shown in Table S1, Supporting Information).

(15) AFM consistently revealed the formation of spherical or oval aggregates of **4** with diameters ranging from 80 to 100 nm, as in the case of probe **1**. Moreover, aggregates of **4** were also observed after addition of hCAI, and the diameters slightly increased (ranging from 100 to 150 nm) in the AFM experiments (Figure S2d, Supporting Information). These results were consisted in the DLS measurements.

(16) Green, N. M. *Biochem. J.* **1963**, *89*, 585.

(17) Matthews, D. A.; Alden, R. A.; Bolin, J. T.; Freer, S. T.; Hamlin, R.; Xuong, N.; Kraut, J.; Poe, M.; Williams, M.; Hoogsteen, K. *Science* **1977**, *197*, 452.

(18) In our previous reports, avidin probe **6** has been evaluated in the buffer with higher ionic strength (500 mM NaCl)[7a] for enhancing the degree of aggregation.

(19) The detection limit of hCAI with probe **12** was less than 2.5 μM, which was at least 2-fold lower than that of probe **1** (5 μM).[7a]

(20) We could not obtain any clear images from the sample containing probe **13** (F = 1) and hCAI, despite accumulation for 3 h.

(21) Chazalette, C.; Masereel, B.; Rolin, S.; Thiry, A.; Scozzafava, A.; Innocenti, A.; Supuran, C. T. *Bioorg. Med. Chem. Lett.* **2004**, *14*, 5781.